THE JOURNAL OF PHYSICAL CHEMISTRY B
A JOURNAL OF THE AMERICAN CHEMICAL SOCIETY

pubs.acs.org/JPCB

Article

Physics-Based Machine Learning to Predict Hydration Free Energies for Small Molecules with a Minimal Number of Descriptors: Interpretable and Accurate

Ajeet Kumar Yadav,[†] Marvin V. Prakash,[†] and Pradipta Bandyopadhyay*

Cite This: https://doi.org/10.1021/acs.jpcb.4c07090

Read Online

ACCESS | Metrics & More | Article Recommendations | Supporting Information

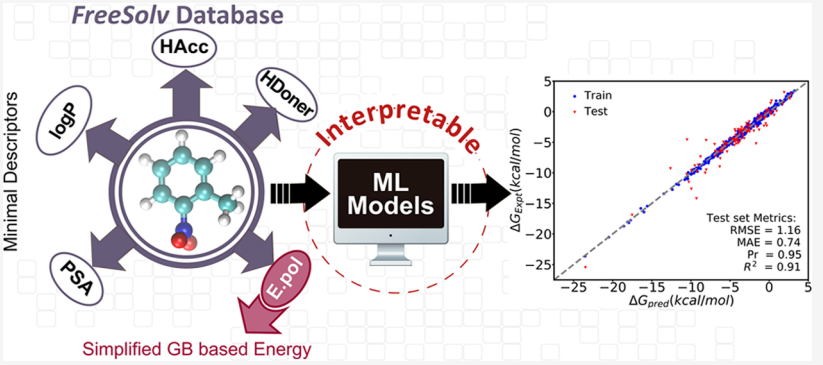

ABSTRACT: Hydration free energy (HFE) of molecules is a fundamental property having importance throughout chemistry and biology. Calculation of the HFE can be challenging and expensive with classical molecular dynamics simulation-based approaches. Machine learning (ML) models are increasingly being used to predict HFE. Although the accuracy of ML models for data sets for small molecules is impressive, these models suffer from lack of interpretability. In this work, we have developed a physics-based ML model with only six descriptors, which is both accurate and fully interpretable, and applied it to a database for small molecule HFE, *FreeSolv*. We evaluated the electrostatic energy by an approximate closed form of the Generalized Born (GB) model and polar surface area. In addition, we have log *P* and hydrogen bond acceptor and donors as descriptors along with the number of rotatable bonds. We have used different ML models, such as random forest and extreme gradient boosting. The best result from these models has a mean absolute error of only 0.74 kcal/mol. The main power of this model is that the descriptors have clear physical meaning, and it was found that the descriptor describing the electrostatics and the polar surface area, followed by the hydrogen bond donors and acceptors, are the most important factors for the calculation of hydration free energy.

INTRODUCTION

Solvation free energy is one of the key quantities in chemistry and biology as most of the molecular phenomena occur in different solvents.[1,2] Water being the most versatile solvent, determination or calculation of hydration free energy (HFE) is the most important step in understanding any complex process. The calculation of HFE is typically done using either a quantum mechanical description of the solute in a dielectric continuum[3−8] or a classical description of the solute where water is treated either with explicit models[9−14] or implicit models (which are mostly dielectric continuum).[10,15−17] The classical force fields are usually used for macromolecules, and for small molecules interacting with macromolecules, classical force fields are used for compatibility. Henceforth, all discussions on the calculation of hydration free energy will be with classical models. Although the physics-based methods are well developed, there are outstanding issues in getting accurate solvation free energy, and it has been an active area of new developments and improvements.[11,18−20] The most rigorous calculations are alchemical methods like thermodynamic integration[21,22] and free energy perturbation.[23] However, these calculations are time-consuming and, generally speaking, are not suitable for a large set of molecules.

Continuum solvent models are often preferred methods when dealing with a larger number of small molecules, which is typical in a drug design project. The Poisson−Boltzmann (PB) and Generalized Born (GB) are the two most common models used in continuum solvent models. In the PB approach, PB eq (or Poisson eq in the absence of any salt concentration) is

Received: October 18, 2024
Revised: January 3, 2025
Accepted: January 7, 2025

solved by defining an interior dielectric constant for the solute and an external dielectric constant for the solvent. The Generalized Born approach also defines internal and external dielectric constants; however, here no electrostatic equation is solved, rather an expression, obtained from the generalization of the Born equation for a single ion, is evaluated.[15,24,25] In both PB and GB approaches, the molecular surface area is calculated, and in GB, the so-called Born radii are calculated, which can be time-consuming. Also, there are some inherent limitations for continuum models, as they neglect the molecular nature of water. There have been several attempts to build cluster-continuum models.[26,27]

From an entirely different perspective, several machine learning (ML) models are developed, in the last couple of years,[28−39] to predict solvation free energy using experimental data in the *FreeSolv* database.[9] The faster speed of ML models compared to physics-based models is advantageous and can be used for large databases of small molecules used in drug discoveries. However, ML models often suffer from a lack of interpretability, and the reasons why they work (or do not work) are often not clear. There have been attempts to define descriptors with clear physical meaning. For instance, Zhang et al. used electron density (obtained from quantum mechanical calculations) based descriptors.[37] In some of the other representative works, Alibakhshi and Hartke have combined ML models with PCM model to predict solvation free energy in different solvents using the components of the PCM calculations as the features of the ML model,[32] Pattnaik et al. have developed an ML model to predict relative solvation free energy in 41 solvents.[38] Vyboishchikov has developed a few NN-based models based on the GB model of solvation.[39−41] The effective Born radii and charges are used as the features in these models. Machine learning has also been used to predict the HFE obtained from molecular dynamics (MD) simulation-based methods.[30]

In the current work, our motivation is to use a minimal number of physically interpretable and simple descriptors for predicting HFE. Starting from the GB expression and with an approximate analytical calculation of Born radii,[25] we evaluate the HFE (after adding five more descriptors) and got accuracy almost as good as the paper by Zhang et al.[37] for the *FreeSolv* data set. The power of our method is that it is completely physics-based and hence fully interpretable. It has only six descriptors, an electrostatics term (GB term summed with Coulomb electrostatic), polar surface area, number of donor and acceptor atoms, log *P*, and the number of rotatable bonds. We have used four different models, namely, Random Forest (RF), Extreme Gradient Boosting (XGBoost), Gradient Boosting (GradBoost), and Light Gradient Boosting Machine (LightGBM). Our best result is a mean absolute error (MAE) of 0.74 kcal/mol comparable to the work of Zhang et al.[37] This method can be used for large data sets used in drug designing and the reason for specific HFE values can be understood clearly as opposed to most of the ML models.

METHODOLOGY

Database Description. The experimental hydration free energy database, *FreeSolv*, prepared by Mobley et al.,[9] has been widely used and benchmarked by various physical solvation models as well as machine learning (ML) and deep learning models. The *FreeSolv* database has 643 small organic molecules with their experimental HFE and SMILES (simplified molecular-input line-entry system). The database also includes the calculated HFE, enthalpy, and entropy data from explicit molecular dynamics simulations. These calculations utilized the GAFF force field,[42] AM1-BCC partial charges,[43,44] and the TIP3P water model.[45] The experimental HFE values have mean and standard deviation of −3.82 and 4.84 kcal/mol, respectively. We have divided the total data set into nine different groups based on the functional group or presence of a specific atom in the molecule. The eight groups are *Alkanol, Alkanone, Alkene, Alkyl Alkanoate, Halo Alkane, Aromatic, Aliphatic cyclic, N-based Aliphatic*, and the ninth, *misc*, is the group for molecules that do not come under any of the previous eight groups. We have assessed the performances of our models both for the whole data set and these different groups.

Descriptor Generation. One of the primary objectives of this work is to utilize a minimal number of descriptors while ensuring that they possess physical interpretability. To achieve this, we have used only six descriptors: polar surface area, hydrogen bond donors, hydrogen bond acceptors, the number of rotatable bonds, log *P*, and an electrostatic term which we call the *pol term* (GB term summed with Coulomb electrostatic). The first five descriptors were calculated using the RDKit[46] package in Python, while the last descriptor is calculated as described below.[25]

The simplified polar energy is the sum of two terms, the Coulombic electrostatic energy and a Generalized Born energy term. The Generalized Born energy term is calculated by the Generalized Born equation as follows:[24]

$$\Delta G_{\text{pol}} = -\frac{1}{2}\left(1 - \frac{1}{\epsilon_{\text{w}}}\right)\sum_{i<j}\frac{q_i q_j}{f_{\text{GB}}} \quad (1)$$

where ϵ_{w} is the dielectric constant of water (the process being moving a solute from vacuum to water), q_i and q_j are the charges of atoms i and j, respectively, and f_{GB} is a function, dependent on the distance between the atoms i and j, that interpolates between the distance r_{ij} and the Born radii. The most widely used functional form of f_{GB} is given below[24]

$$f_{\text{GB}} = \left[r_{ij}^2 + R_i R_j \exp\left(-\frac{r_{ij}}{4R_i R_j}\right)\right]^{1/2} \quad (2)$$

where R_i and R_j are the effective Born radii of atoms i and j, respectively. The main challenge in the implementation of the GB model is the calculation of the effective Born radius.

Approximate Analytical Evaluation of Born Radius. When the accessible surfaces of the atoms of a molecule are nonoverlapping, then it can be shown that the following (eq 3) is an analytical expression for Born radius, a_i being the sum of the radii of the atom i and water.[25]

$$R_i^{-1} = a_i^{-1} - \sum_j \frac{a_j}{2(r_{ij}^2 - a_j^2)} - \frac{1}{4r_{ij}}\log\left(\frac{r_{ij} - a_j}{r_{ij} + a_j}\right) \quad (3)$$

The charge and radius of atoms are taken from the Generalized Amber ForceField (GAFF) force field[42] (water radius was taken as 1.4 Å). Although eq 3 is valid only for nonoverlapping atoms, this can act as an excellent descriptor in an ML model. In the evaluation of eq 3, the numerator of the second term can be negative for overlapping accessible surfaces of the atoms. To circumvent this problem, we have performed the sum over the pairs of atoms with nonoverlapping accessible surfaces only. This approximation provides a fast estimation of

https://doi.org/10.1021/acs.jpcb.4c07090
J. Phys. Chem. B XXXX, XXX, XXX−XXX

the polar part of the solvation free energy. Our results show that using this approximation as a descriptor, ML-based methods perform well for the *FreeSolv* database.

Machine Learning Models. Figure 1 illustrates the workflow for predicting the hydration free energy. It highlights

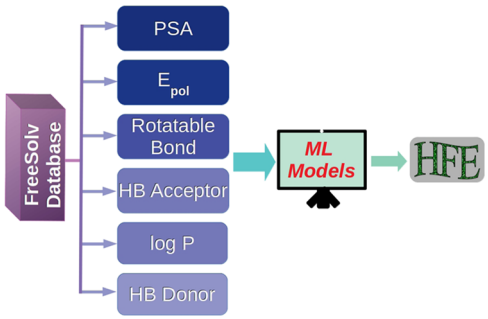

Figure 1. Workflow to predict ΔG_{Hyd} using ML-based models. It involves the calculation of descriptors, ML model training, and then predicting HFE.

that the six descriptors are calculated for the *FreeSolv* database first. Then, different ML methods are trained and HFE is predicted. Regression algorithms will enable ML models to make predictions based on the information represented by each chemical feature. After calculating RDKit descriptors, the database was divided into two subsets. We used an 80:20 split to divide the data set into training and testing sets, ensuring that this ratio was consistently maintained across the nine predefined groups. These subsets were utilized to develop, train, and statistically evaluate the model using different ML algorithms. We applied `StandardScaler` to standardize the features, which helps improve model performance by scaling data to have a mean of zero and a standard deviation of one. This ensures that all features contribute equally to the model training process and improve convergence during optimization. After these preprocessing steps, different machine learning models are trained on the training set to learn the crucial relationships for making predictions and then tested on the unseen testing set to assess the prediction accuracy.

We employed four different machine learning models: Random Forest (RF),[47] Extreme Gradient Boosting (XGBoost),[48] Gradient Boosting (GradBoost),[49] and Light Gradient Boosting Machine (LightGBM).[50] These models are trained on the training set to learn the crucial relationships of the descriptors with the HFE that is the target property. Although all of the above four machine learning models—RF, XGBoost, GradBoost, and LightGBM—use ensemble techniques, their approaches to prediction differ. Random Forest is a bagging-based technique that builds multiple decision trees independently by averaging their predictions to reduce variance and improve stability. Gradient Boosting applies a boosting strategy to further train the weak learners one after another in a sequence to minimize the loss function while correcting the mistakes of the preceding one. The other two methods, XGBoost, and LightGBM, are more advanced versions of the Gradient Boosting algorithm. XGBoost uses regularization, parallel processing, and tree-trimming methods to overcome the overfitting. LightGBM, another variant of Gradient Boosting, was developed to handle large amounts of data; it uses leaf-wise growth and histogram-based learning to speed up and reduce memory usage. Collectively, these models use various techniques to merge decision trees to balance prediction accuracy and computing time. We have trained and tested our ML models on two classes of data: (1) full data set and (2) without outliers. We have used the interquartile range (IQR) method to define outliers in the experimental hydration free energy, with bounds set at $Q_1 - 1.5 \times \text{IQR}$ and $Q_3 + 1.5 \times \text{IQR}$. Q1 and Q3 are the first and third quartiles, respectively. This leaves 628 molecules in the second data set.

We also utilized `GridSearchCV` with 5-fold cross-validation to optimize the hyperparameters of our model. This method involves systematically searching through a grid of hyperparameter values to identify the best settings for our model. In conjunction with 5-fold cross-validation, the data set is divided into 5 folds. The model is trained on 4 folds for each hyperparameter combination and evaluated on the remaining fold. This process is repeated 5 times, each time using a different fold as the test set. We ensure that the selected hyperparameters provide robust and generalizable model performance by averaging the performance across these iterations. In Table S1 in the SI, we have listed the optimized parameters of the four models we have used.

To evaluate the performance of our model, we employed several metrics: root mean square error (RMSE), mean absolute error (MAE), Pearson correlation coefficient (*Pr*), and R^2 score. RMSE and MAE provide insights into the magnitude of prediction errors, while *Pr* assesses the strength of the linear relationship between observed and predicted values, and R^2 indicates the proportion of variance explained by the model. These metrics were used to evaluate our model's accuracy and robustness rigorously, and the results were compared with those from other studies to benchmark our model's performance against existing methods. The feature importance for each descriptor was calculated by using the mean decrease of impurity.

RESULTS AND DISCUSSION

Performance of the Simplified GB Model. First, we assessed the performance of the approximated GB model alone in Figure 2. The figure shows that the model has relatively high values of RMSE and MAE, indicating that this model alone is not accurate enough and needs further refinement.

Machine Learning-Based Model Performance. To select the appropriate model for our study, we have compared the hydration free energy prediction performance of the random forest (RF) and XGBoost models in Figure 3.

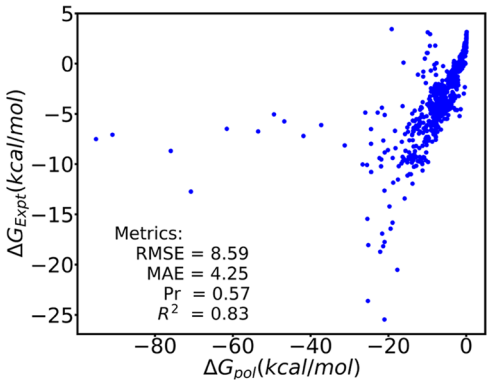

Figure 2. Scatter plot compares the experimental hydration free energy with the predicted values.

https://doi.org/10.1021/acs.jpcb.4c07090
J. Phys. Chem. B XXXX, XXX, XXX−XXX

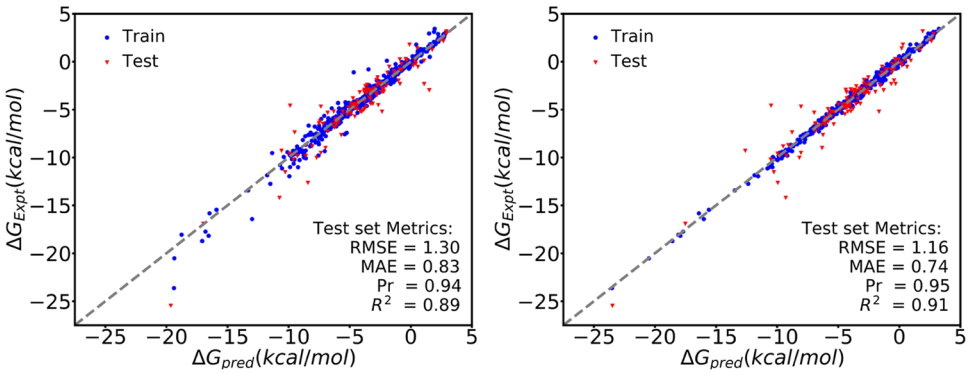

Figure 3. Comparison of hydration free energy predictions using the Random Forest (left) and Extreme Gradient Boosting (right) models for the full data set.

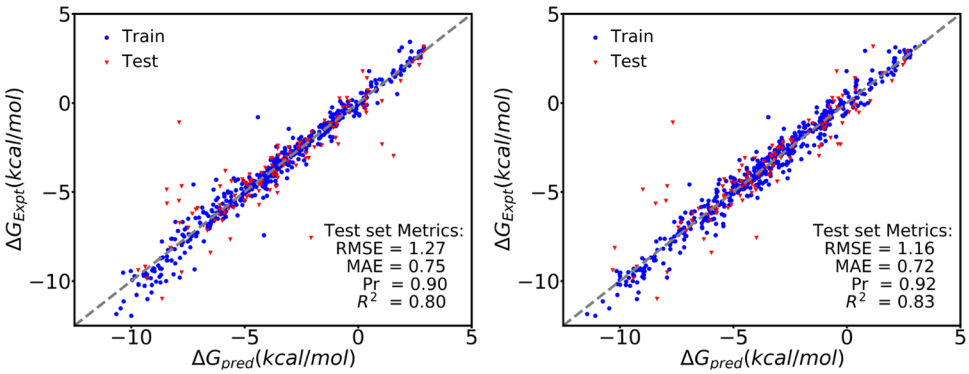

Figure 4. Comparison of hydration free energy predictions by Random Forest (left) and Extreme Gradient Boosting (right) models for the data set without outliers.

Performances of the other two models are shown in Figure S1 in the Supporting Information (SI). For the RF model, the test set root mean squared error (RMSE) is 1.30 kcal/mol and the coefficient of determination (R^2) is 0.89, indicating that the model explains approximately 89% of the variance in the test set. The Pearson correlation coefficient (Pr) is 0.94, demonstrating a strong linear correlation between the predicted and experimental HFE values. The mean absolute error (MAE) of 0.83 kcal/mol reflects that the model provides accurate predictions overall.

In comparison, the XGBoost model outperforms Random Forest, with a lower RMSE of 1.16 kcal/mol and a higher R^2 value of 0.91, explaining about 91% of the variance in the test set. The Pearson correlation coefficient for XGBoost is Pr = 0.95, indicating a very strong linear relationship between the predicted and experimental values. The MAE of 0.74 kcal/mol confirms XGBoost's improved predictive accuracy and precision compared to Random Forest. Both models exhibit strong agreement between predicted and experimental values, with data points clustered along the diagonal line in the parity plots. However, XGBoost shows a more concentrated distribution, particularly at lower ΔG values, suggesting that it provides a better fit overall. The Gradient Boosting model and LightGBM, shown in Figure S1 in the SI, perform comparably with the Random Forest and XGBoost models. For Gradient Boosting, with an RMSE of 1.28 kcal/mol and R^2 = 0.89, it explains about 89% of the variance in the test set, similar to Random Forest. The Pearson correlation coefficient of Pr = 0.95 indicates a strong linear relationship between the predicted and experimental values. The MAE of 0.81 kcal/mol highlights its reliable predictive performance. On the other hand, LightGBM has an MAE of 0.84 kcal/mol. The analysis demonstrates that XGBoost and Gradient Boosting outperform Random Forest and LightGBM, with XGBoost offering the most accurate predictions overall.

All of the models display slight deviations, indicating potential areas for further improvement. To overcome the deviations, we retrained the models to assess their performance without outliers. We have compared the hydration free energy prediction performance of the RF and XGBoost models without outliers in Figure 4. Performances of the other two models are shown in Figure S2 in the SI. The Random Forest model had an RMSE of 1.27 kcal/mol, an MAE of 0.75 kcal/mol, an R^2 of 0.80, and a Pearson correlation coefficient of 0.90. Despite the removal of outliers, the model's performance slightly decreased compared to the original data set, especially in terms of the correlations i.e., R^2 value and Pr. However, the XGBoost model maintained strong predictive performance without outliers, with an improved RMSE of 1.16 kcal/mol, an R^2 value of 0.83, and a Pearson correlation coefficient of 0.92. The MAE for XGBoost decreased to 0.72 kcal/mol, reflecting only a slight increase in accuracy compared to its performance on the full data set. The LightGBM model's performance was comparable to Random Forest, with an RMSE of 1.27 kcal/mol, an MAE of 0.78 kcal/mol, an R^2 value of 0.80, and a Pearson correlation coefficient of Pr = 0.90. In contrast, the Gradient Boosting model performed significantly better without outliers, achieving an RMSE of 1.11 kcal/mol and an R^2 value of 0.85, along with a Pearson correlation coefficient of Pr = 0.92. The MAE for this model was 0.70 kcal/mol, indicating improved accuracy compared to the full data set. While LightGBM showed similar results to Random Forest, it

https://doi.org/10.1021/acs.jpcb.4c07090
J. Phys. Chem. B XXXX, XXX, XXX−XXX

performed slightly worse compared to Gradient Boosting and XGBoost in terms of both RMSE and MAE. The removal of outliers generally led to improved accuracy for most models, making Gradient Boosting the strongest performance on this cleaner data set. Table 1 summarizes the metrics for the RF, GradBoost, XGBoost, and LightGBM models with and without outliers.

Table 1. Performance Metrics for Models with and without Outliers (RF: Random Forest, GradBoost: Gradient Boosting, XGBoost: Extreme Gradient Boosting, LGBM: Light Gradient Boosting Machine)

with outliers				
	RF	GradBoost	XGBoost	LightGBM
RMSE (train/test)	0.60/1.30	0.51/1.28	0.47/1.15	0.93/1.32
MAE (train/test)	0.37/0.83	0.38/0.81	0.34/0.74	0.64/0.84
R^2 (train/test)	0.98/0.89	0.98/0.89	0.98/0.91	0.94/0.88
R_p (train/test)	0.99/0.94	0.99/0.94	0.99/0.96	0.97/0.94
without outliers				
	RF	GB	XGB	LGBM
RMSE (train/test)	0.56/1.27	0.68/1.11	0.56/1.16	0.85/1.27
MAE (train/test)	0.37/0.75	0.49/0.70	0.41/0.72	0.60/0.78
R^2 (train/test)	0.97/0.80	0.96/0.85	0.97/0.83	0.93/0.80
R_p (train/test)	0.99/0.90	0.98/0.92	0.99/0.92	0.97/0.90

Descriptor Performance. The feature importance for the different models highlights the varying roles each descriptor plays in predicting the target variable. We have shown the feature importance for RF and XGBoost in Figure 5 and for Gradient Boosting and LightGBM in Figure S3 in the SI. In both the Random Forest and Gradient Boosting models, the polar surface area (psa) emerges as the most important feature, contributing around 50%, followed by the *pol term*, which accounts for approximately 30%. It is to be noted that polar surface area and nonpolar surface area are complementary features. In this work, we have taken PSA; however, taking PSA as a feature implicitly includes nonpolar surface area also. Hence, the importance of PSA as a feature indicates the importance of the polarity of surface areas in general. These polarities of surface area and the pol term dominate the prediction capabilities of these models, suggesting that molecular surface properties play a crucial role in the prediction task. Other descriptors like the number of hydrogen bond donors (*n_donors*), rotatable bonds (nrotb), acceptors (*n_acceptors*), and log *P* contribute significantly less. This highlights a strong dependence on molecular polarity and surface area in these ensemble tree-based models.

Interestingly, the XGBoost model demonstrates a different feature importance distribution where the number of acceptors (*n_acceptors*) becomes the most dominant feature, contributing 30% to the predictions. *Pol term* and psa play smaller but still significant roles, contributing around 18−22%. This indicates that the XGBoost model is more sensitive to hydrogen bond acceptor characteristics than the other models. LightGBM also highlights psa, log *P*, and *pol term* as the most critical features. These results suggest that while the molecular surface and polarity remain crucial across models, each model places a different emphasis on these features based on their algorithmic structure.

To understand the range of applicability of the descriptors, we have performed the Kernel density examination (KDE) and put it in the SI. One of the purposes for KDE is to see the range of features used to train the model and make judgment on whether this model will be stable if range of features are exceeded in a larger data set or in this case for larger molecules. From the figures few points emerge. For instance, the increase in the number of rotatable bonds increases the conformational entropy of the molecule and one structure, as used in this study, may not be appropriate to prediction hydration free energy. However, the bigger issue, which is not clear from the KDE, is that the approximate closed expression for Born Radii will be a weaker one as the size and complexity of the molecules increase.

Comparison with Other ML Models Used for FreeSolv Data Set. We compared our models with previous models trained on the *FreeSolv* database. In comparison to several previous models, such as CIGIN[34] (0.76), MLSolvA[33] (0.76), and MoleculeNet[29] (1.15), our XGB model achieves a lower test MAE (0.74). At the same time, there are models (e.g., the A3D-PNAConv-FT[35] with the MAE of 0.42) having lower MAE than ours. However, essentially all previous models for predicting HFE use complex descriptors (and more complex predictors), making the interpretation difficult. For instance, Lim and Jung[33] have expressed hydration free energy as a sum over atomistic contributions, while Pathak et al.[34] have represented molecules as graphs and both atom and bond features are used. In our model, the nonadditivity of hydration free energy is already taken in the GB term, and that is the main reason that our model achieved excellent performance with only six descriptors.

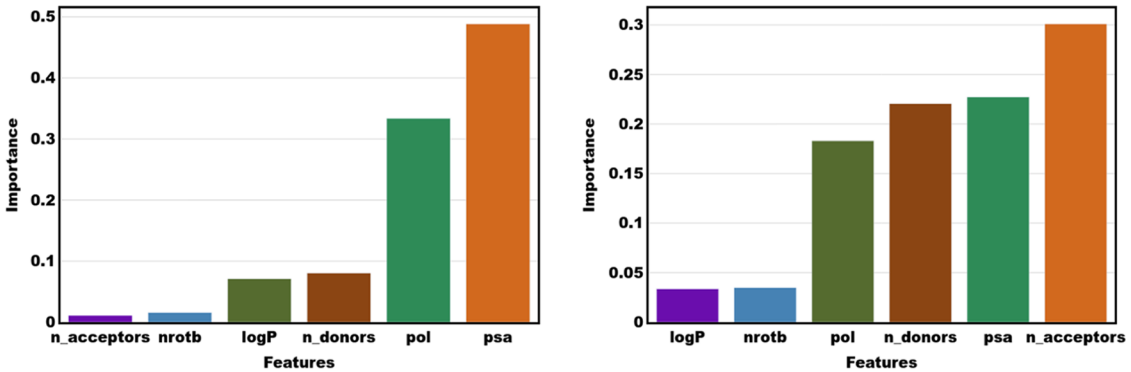

Figure 5. Comparison of feature importance for Random Forest (left) and XGBoost (right) models. The bars represent the relative importance of each feature in predicting the target variable.

https://doi.org/10.1021/acs.jpcb.4c07090
J. Phys. Chem. B XXXX, XXX, XXX−XXX

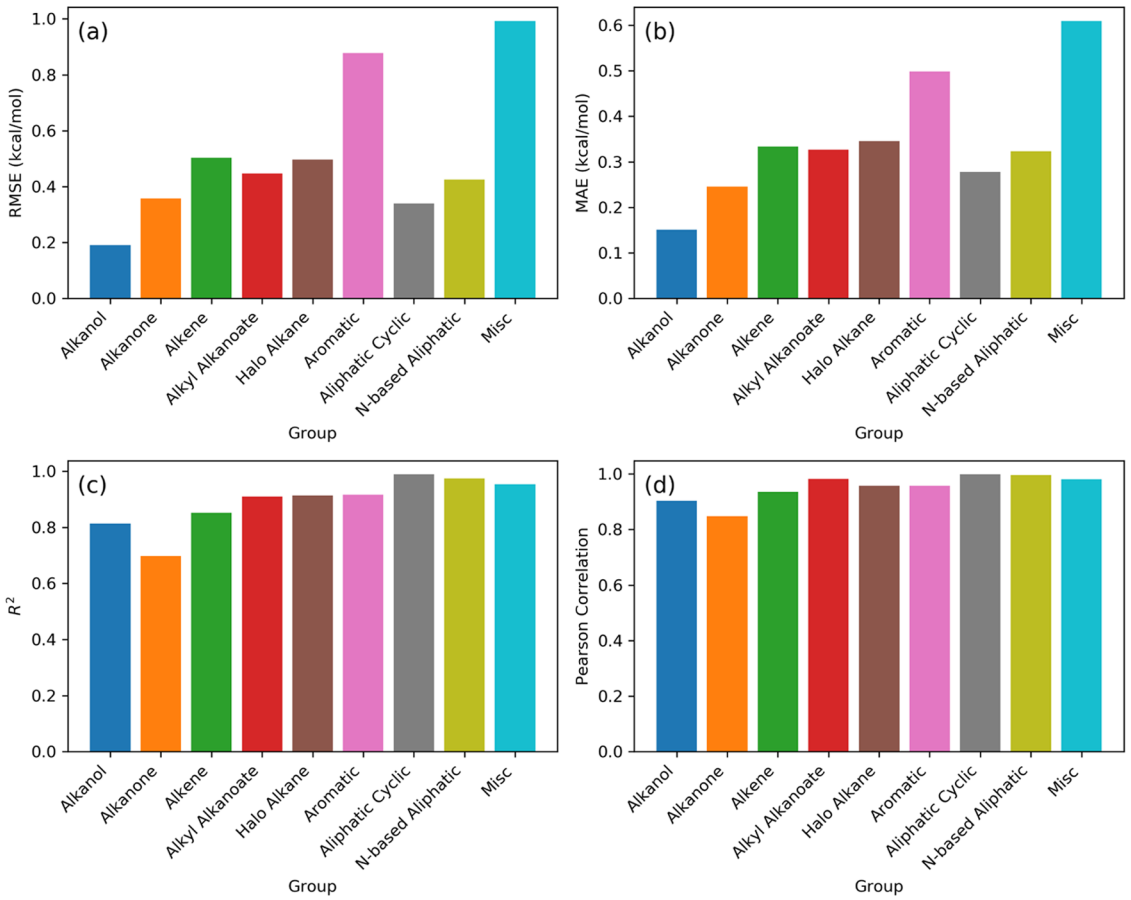

Figure 6. Group-wise performance metrics for the model: (a) root mean square error (RMSE) in kcal/mol, (b) mean absolute error (MAE) in kcal/mol, (c) coefficient of determination (R^2), and (d) Pearson correlation coefficient (Pr). Each bar represents the performance metric for a specific group of compounds, as described in the text.

Performance against Different Functional Groups. We have assessed the performance of our models on the nine groups defined in the Methodology section. Figure 6 shows the performance metrics for the RF regression model for the nine groups. The RMSE and MAE for the ninth group i.e., misc (molecules not categorized in any of the previous eight groups) show the highest deviation in the prediction with their values of 0.99 and 0.61 kcal/mol, respectively. But the correlation metrics i.e., R^2 and Pr show different behavior than the error metrics. The correlation metrics for this group (R^2 = 0.95 and Pr = 0.98) indicate that this group's performance closely agrees with experimental hydration free energy. These two contradicting metrics show that there is a systematic error in the model in both the training and testing phases. The same contradicting trend is also observed in the case of *aromatic* group. Except for these two groups, our models perform well across different groups with relatively low RMSE (less than 0.53 kcal/mol) and low MAE (less than 0.36 kcal/mol). For the correlation metrics, except for *alkanone* and *alokanol* groups, all other groups are highly correlated with their corresponding experimental hydration free energy. The R^2 is always more than 0.85, and Pr is always greater than 0.93 except for *alkanone* and *alokanol* groups, which signifies the performance of our model across the groups.

CONCLUSIONS

In this work, we have developed a physics-based and interpretable machine learning model for predicting the hydration free energy of small molecules with only six descriptors. Our results compare well with other works with this data set. However, the advantage of our method is that the results are fully interpretable, which is often an issue with the ML models. Our models perform well across different chemical groups, signifying their applicability to larger databases such as those used in drug discoveries.

ASSOCIATED CONTENT

Data Availability Statement

The codes used in this work are available at GitHub repository: https://github.com/M4Marvin/Hydration_Free_Energies_Prediction.

Supporting Information

The Supporting Information is available free of charge at https://pubs.acs.org/doi/10.1021/acs.jpcb.4c07090.

Additional plots comparing hydration free energy using Gradient Boosting and Light Gradient Boosting methods; kernel density analysis for experimental hydration free energy and for the six descriptors (PDF)

AUTHOR INFORMATION

Corresponding Author

Pradipta Bandyopadhyay − *School of Computational and Integrative Sciences, Jawaharlal Nehru University, New Delhi*

https://doi.org/10.1021/acs.jpcb.4c07090
J. Phys. Chem. B XXXX, XXX, XXX−XXX

110067, India; orcid.org/0000-0001-6343-623X; Email: praban07@gmail.com

Authors

Ajeet Kumar Yadav − *School of Computational and Integrative Sciences, Jawaharlal Nehru University, New Delhi 110067, India*

Marvin V. Prakash − *School of Computational and Integrative Sciences, Jawaharlal Nehru University, New Delhi 110067, India*

Complete contact information is available at: https://pubs.acs.org/10.1021/acs.jpcb.4c07090

Author Contributions

†A.K.Y. and M.V.P. contributed equally to this work.

Notes

The authors declare no competing financial interest.

■ ACKNOWLEDGMENTS

This work was supported by a MATRICS grant from SERB (MTR/2021/000365) awarded to P.B. This work was also partially supported by grants from the DBT (BT/PR/40251/BITS/137/11/2021) awarded to the Centre for Computational Biology and Bioinformatics, Jawaharlal Nehru University, and by the Indo-Slovenia bilateral research grant from DST (DST/ICD/Indo-Slovenia/2022/02(G)). The authors thank Prof. Tomaz Urbic for insightful discussions.

■ REFERENCES

(1) Brini, E.; Fennell, C. J.; Fernandez-Serra, M.; Hribar-Lee, B.; Luksic, M.; Dill, K. A. How water's properties are encoded in its molecular structure and energies. *Chem. Rev.* **2017**, *117*, 12385−12414.

(2) Perlovich, G. L. Thermodynamic approaches to the challenges of solubility in drug discovery and development. *Mol. Pharmaceutics* **2014**, *11*, 1−11.

(3) Mennucci, B. Polarizable continuum model. *WIREs Comput. Mol. Sci.* **2012**, *2*, 386−404.

(4) Klamt, A. The COSMO and COSMO-RS solvation models. *WIREs Comput. Mol. Sci.* **2011**, *1*, 699−709.

(5) Mennucci, B.; Tomasi, J. Continuum solvation models: A new approach to the problem of solute's charge distribution and cavity boundaries. *J. Chem. Phys.* **1997**, *106*, 5151−5158.

(6) Luukkonen, S.; Belloni, L.; Borgis, D.; Levesque, M. Predicting hydration free energies of the FreeSolv database of drug-like molecules with molecular density functional theory. *J. Chem. Inf. Model.* **2020**, *60*, 3558−3565.

(7) Voityuk, A. A.; Vyboishchikov, S. F. A simple COSMO-based method for calculation of hydration energies of neutral molecules. *Phys. Chem. Chem. Phys.* **2019**, *21*, 18706−18713.

(8) Kříž, K.; Rezac, J. Reparametrization of the COSMO solvent model for semiempirical methods PM6 and PM7. *J. Chem. Inf. Model.* **2019**, *59*, 229−235.

(9) Mobley, D. L.; Guthrie, J. P. FreeSolv: a database of experimental and calculated hydration free energies, with input files. *J. Comput.-Aided Mol. Des.* **2014**, *28*, 711−720.

(10) Shivakumar, D.; Deng, Y.; Roux, B. Computations of absolute solvation free energies of small molecules using explicit and implicit solvent model. *J. Chem. Theory Comput.* **2009**, *5*, 919−930.

(11) Shivakumar, D.; Harder, E.; Damm, W.; Friesner, R. A.; Sherman, W. Improving the prediction of absolute solvation free energies using the next generation OPLS force field. *J. Chem. Theory Comput.* **2012**, *8*, 2553−2558.

(12) Nerenberg, P. S.; Jo, B.; So, C.; Tripathy, A.; Head-Gordon, T. Optimizing solute−water van der Waals interactions to reproduce solvation free energies. *J. Phys. Chem. B* **2012**, *116*, 4524−4534.

(13) Riquelme, M.; Lara, A.; Mobley, D. L.; Verstraelen, T.; Matamala, A. R.; Vohringer-Martinez, E. Hydration free energies in the FreeSolv database calculated with polarized iterative Hirshfeld charges. *J. Chem. Inf. Model.* **2018**, *58*, 1779−1797.

(14) Heyden, M. Disassembling solvation free energies into local contributions−Toward a microscopic understanding of solvation processes. *WIREs Comput. Mol. Sci.* **2019**, *9*, No. e1390.

(15) Onufriev, A. V.; Case, D. A. Generalized Born implicit solvent models for biomolecules. *Annu. Rev. Biophys.* **2019**, *48*, 275−296.

(16) Tan, C.; Yang, L.; Luo, R. How well does Poisson- Boltzmann implicit solvent agree with explicit solvent? A quantitative analysis. *J. Phys. Chem. B* **2006**, *110*, 18680−18687.

(17) Aguilar, B.; Onufriev, A. V. Efficient computation of the total solvation energy of small molecules via the R6 generalized Born model. *J. Chem. Theory Comput.* **2012**, *8*, 2404−2411.

(18) Lang, E. J. M.; Baker, E. G.; Woolfson, D. N.; Mulholland, A. J. Generalized Born implicit solvent models do not reproduce secondary structures of de novo designed Glu/Lys peptides. *J. Chem. Theory Comput.* **2022**, *18*, 4070−4076.

(19) Bass, L.; Elder, L. H.; Folescu, D. E.; Forouzesh, N.; Tolokh, I. S.; Karpatne, A.; Onufriev, A. V. Improving the Accuracy of Physics-Based Hydration-Free Energy Predictions by Machine Learning the Remaining Error Relative to the Experiment. *J. Chem. Theory Comput.* **2024**, *20*, 396−410.

(20) He, X.; Man, V. H.; Yang, W.; Lee, T.-S.; Wang, J. A fast and high-quality charge model for the next generation general AMBER force field. *J. Chem. Phys.* **2020**, *153*, No. 114502.

(21) Martins, S. A.; Sousa, S. F.; Ramos, M. J.; Fernandes, P. A. Prediction of solvation free energies with thermodynamic integration using the general amber force field. *J. Chem. Theory Comput.* **2014**, *10*, 3570−3577.

(22) Yu, Z.; Batista, E. R.; Yang, P.; Perez, D. Acceleration of Solvation Free Energy Calculation via Thermodynamic Integration Coupled with Gaussian Process Regression and Improved Gelman−Rubin Convergence Diagnostics. *J. Chem. Theory Comput.* **2024**, *20*, 2570−2581.

(23) Zwanzig, R. W. High-temperature equation of state by a perturbation method. I. Nonpolar gases. *J. Chem. Phys.* **1954**, *22*, 1420−1426.

(24) Still, W. C.; Tempczyk, A.; Hawley, R. C.; Hendrickson, T. Semianalytical treatment of solvation for molecular mechanics and dynamics. *J. Am. Chem. Soc.* **1990**, *112*, 6127−6129.

(25) Bashford, D.; Case, D. A. Generalized born models of macromolecular solvation effects. *Annu. Rev. Phys. Chem.* **2000**, *51*, 129−152.

(26) Bandyopadhyay, P.; Gordon, M. S. A combined discrete/continuum solvation model: application to glycine. *J. Chem. Phys.* **2000**, *113*, 1104−1109.

(27) Bandyopadhyay, P.; Gordon, M. S.; Mennucci, B.; Tomasi, J. An integrated effective fragment—-polarizable continuum approach to solvation: Theory and application to glycine. *J. Chem. Phys.* **2002**, *116*, 5023−5032.

(28) Zhang, P.; Shen, L.; Yang, W. Solvation free energy calculations with quantum mechanics/molecular mechanics and machine learning models. *J. Phys. Chem. B* **2019**, *123*, 901−908.

(29) Wu, Z.; Ramsundar, B.; Feinberg, E. N.; Gomes, J.; Geniesse, C.; Pappu, A. S.; Leswing, K.; Pande, V. MoleculeNet: a benchmark for molecular machine learning. *Chem. Sci.* **2018**, *9*, 513−530.

(30) Bennett, W. F. D.; He, S.; Bilodeau, C. L.; Jones, D.; Sun, D.; Kim, H.; Allen, J. E.; Lightstone, F. C.; Ingólfsson, H. I. Predicting small molecule transfer free energies by combining molecular dynamics simulations and deep learning. *J. Chem. Inf. Model.* **2020**, *60*, 5375−5381.

(31) Chen, D.; Gao, K.; Nguyen, D. D.; Chen, X.; Jiang, Y.; Wei, G.-W.; Pan, F. Algebraic graph-assisted bidirectional transformers for molecular property prediction. *Nat. Commun.* **2021**, *12*, No. 3521.

(32) Alibakhshi, A.; Hartke, B. Improved prediction of solvation free energies by machine-learning polarizable continuum solvation model. *Nat. Commun.* **2021**, *12*, No. 3584.

(33) Lim, H.; Jung, Y. MLSolvA: solvation free energy prediction from pairwise atomistic interactions by machine learning. *J. Cheminf.* **2021**, *13*, No. 56.
(34) Pathak, Y.; Mehta, S.; Priyakumar, U. D. Learning atomic interactions through solvation free energy prediction using graph neural networks. *J. Chem. Inf. Model.* **2021**, *61*, 689−698.
(35) Zhang, D.; Xia, S.; Zhang, Y. Accurate prediction of aqueous free solvation energies using 3D atomic feature-based graph neural network with transfer learning. *J. Chem. Inf. Model.* **2022**, *62*, 1840−1848.
(36) Low, K.; Coote, M. L.; Izgorodina, E. I. Explainable solvation free energy prediction combining graph neural networks with chemical intuition. *J. Chem. Inf. Model.* **2022**, *62*, 5457−5470.
(37) Zhang, Z.-Y.; Peng, D.; Liu, L.; Shen, L.; Fang, W.-H. Machine Learning Prediction of Hydration Free Energy with Physically Inspired Descriptors. *J. Phys. Chem. Lett.* **2023**, *14*, 1877−1884.
(38) Pattanaik, L.; Menon, A.; Settels, V.; Spiekermann, K. A.; Tan, Z.; Vermeire, F. H.; Sandfort, F.; Eiden, P.; Green, W. H. ConfSolv: Prediction of Solute Conformer-Free Energies across a Range of Solvents. *J. Phys. Chem. B* **2023**, *127*, 10151−10170.
(39) Vyboishchikov, S. F. Predicting Solvation Free Energies Using Electronegativity-Equalization Atomic Charges and a Dense Neural Network: A Generalized-Born Approach. *J. Chem. Theory Comput.* **2023**, *19*, 8340−8350.
(40) Vyboishchikov, S. F. Dense Neural Network for Calculating Solvation Free Energies from Electronegativity-Equalization Atomic Charges. *J. Chem. Inf. Model.* **2023**, *63*, 6283−6292.
(41) Vyboishchikov, S. F. Solvation Enthalpies and Free Energies for Organic Solvents through a Dense Neural Network: A Generalized-Born Approach. *Liquids* **2024**, *4*, 525−538.
(42) Wang, J.; Wolf, R. M.; Caldwell, J. W.; Kollman, P. A.; Case, D. A. Development and testing of a general amber force field. *J. Comput. Chem.* **2004**, *25*, 1157−1174.
(43) Jakalian, A.; Bush, B. L.; Jack, D. B.; Bayly, C. I. Fast, efficient generation of high-quality atomic charges. AM1-BCC model: I. Method. *J. Comput. Chem.* **2000**, *21*, 132−146.
(44) Jakalian, A.; Jack, D. B.; Bayly, C. I. Fast, efficient generation of high-quality atomic charges. AM1-BCC model: II. Parameterization and validation. *J. Comput. Chem.* **2002**, *23*, 1623−1641.
(45) Jorgensen, W. L.; Chandrasekhar, J.; Madura, J. D.; Impey, R. W.; Klein, M. L. Comparison of simple potential functions for simulating liquid water. *J. Chem. Phys.* **1983**, *79*, 926−935.
(46) Landrum, G. *Rdkit: Open-Source Cheminformatics Software*, 2016.
(47) Ho, T. K. In *Random Decision Forests*, Proceedings of 3rd International Conference on Document Analysis and Recognition; IEEE, 1995; pp 278−282.
(48) Chen, T.; Guestrin, C. In *XGBoost: A Scalable Tree Boosting System*, Proceedings of the 22nd ACM SIGKDD International Conference on Knowledge Discovery and Data Mining; ACM, 2016; pp 785−794.
(49) Natekin, A.; Knoll, A. Gradient boosting machines, a tutorial. *Front. Neurorobotics* **2013**, *7*, No. 21.
(50) Ke, G.; Meng, Q.; Finley, T.; Wang, T.; Chen, W.; Ma, W.; Ye, Q.; Liu, T.-Y. In *Lightgbm: A Highly Efficient Gradient Boosting Decision Tree*, Advances in Neural Information Processing Systems; NIPS, 2017; pp 1−9.

https://doi.org/10.1021/acs.jpcb.4c07090
J. Phys. Chem. B XXXX, XXX, XXX−XXX